

Subspace Clustering by Exploiting a Low-Rank Representation with a Symmetric Constraint

Jie Chen, Zhang Yi*

Machine Intelligence Laboratory, College of Computer Science, Sichuan University, Chengdu 610065, P.R. China

Abstract

In this paper, we propose a low-rank representation with symmetric constraint (LRRSC) method for robust subspace clustering. Given a collection of data points approximately drawn from multiple subspaces, the proposed technique can simultaneously recover the dimension and members of each subspace. LRRSC extends the original low-rank representation algorithm by integrating a symmetric constraint into the low-rankness property of high-dimensional data representation. The symmetric low-rank representation, which preserves the subspace structures of high-dimensional data, guarantees weight consistency for each pair of data points so that highly correlated data points of subspaces are represented together. Moreover, it can be efficiently calculated by solving a convex optimization problem. We provide a rigorous proof for minimizing the nuclear-norm regularized least square problem with a symmetric constraint. The affinity matrix for spectral clustering can be obtained by further exploiting the angular information of the principal directions of the symmetric low-rank representation. This is a critical step towards evaluating the memberships between data points. Experimental results on benchmark databases demonstrate the effectiveness and robustness of LRRSC compared with several state-of-the-art subspace clustering algorithms.

Keywords:

Low-rank representation, subspace clustering, affinity matrix learning, spectral clustering

1. Introduction

In recent years, subspace clustering techniques have attracted much attention from researchers in many areas; for example, computer vision, machine learning, and pattern recognition. Subspace clustering is important to numerous applications such as image representation [1, 2], clustering [3–7], and motion segmentation [8–12]. The generality and importance of subspaces naturally lead to the challenging problem of subspace clustering, where the goal is to simultaneously segment data into clusters that correspond to a low-dimensional subspace. To be more specific, given a set of data points drawn from a mixture of subspaces, the task is to segment all data points into their respective subspaces.

When we consider of subspace clustering in real applications, there is a large amount of high-dimensional data available; for example, digital images, video surveillance, and traffic monitoring. High-dimension data increase the computational cost of algorithms and have a negative effect on performance because of noise and corrupted observations. It is typical to impose an assumption that the high-dimensional data are approximately drawn from a union of multiple subspaces. This assumption is reasonable because data in a class can be well represented by a low-dimensional subspace of the high-dimensional ambient space. In fact, high-dimensional data often have a

smaller intrinsic dimension. Examples of high-dimensional data that lie in a low-dimensional subspace of the ambient space include images of an individual’s face captured under various laboratory-controlled lighting conditions, handwritten images of a digit with different rotations, translations, and thicknesses, and feature trajectories of a moving object in a video [13, 14]. This has motivated the development of a number of techniques [15–21] for finding and exploiting low-dimensional structures in high-dimensional data.

Principal component analysis (PCA) [22] can reveal the hidden structures of data from a single low-dimensional subspace of a high-dimensional space, and can be stably and efficiently computed using singular value decomposition (SVD). However, a single subspace is often not adequate for describing data [2, 4]. In fact, data often lie close to a union of low-dimensional subspaces. A number of methods have been devised to exactly solve the subspace clustering problem [23]. Subspace clustering methods can be roughly divided into statistical learning based [24], factorization based [25–27], algebra based [28], iterative [29], and spectral-type based methods [4, 5, 12, 30, 31].

Statistical learning based approaches such as random sample consensus (RANSAC) [24] assume that a set of independent samples is drawn from a mixture of probabilistic distributions. RANSAC can deal with noise and outliers, and it does not need to know the number of subspaces. However, it requires that the dimension of the subspaces be known and equal. In addition, a major disadvantage of RANSAC is that there is no upper bound on the time it takes to tune parameters. This seriously limits

*Corresponding author

Email address: zyiscu@gmail.com (Zhang Yi)

its practical applicability. Matrix factorization based methods decompose the data matrix into the product of two matrices, and reveal clusters using the structure of the factorization results. In particular, the shape interaction matrix [25] can be used for spectral clustering by factorizing the data matrix. Generalized principal component analysis [28] is a popular algebraic method that simultaneously clusters the data into multiple subspaces, and finds a low-dimensional subspace that fits each group of points. Iterative methods such as K-subspaces [29] alternate between assigning points to the nearest subspaces and fitting a subspace to each cluster. These methods can produce good results under the assumption that data are strictly drawn from linearly independent subspaces. However, an increase in difficulty is in part caused by the data not strictly following subspace structures (because of noise and corruptions), and can lead to indistinguishable subspace clustering. Therefore, subspace clustering algorithms that take into account the multiple subspace structure of high-dimensional data are required.

Some work on sparse representation theory and rank minimization [4, 5, 30, 32–35] has recently been proposed to alleviate these drawbacks. Effective approaches to subspace clustering called spectral-type based methods have been developed. These methods typically perform subspace clustering in two stages: they first learn an affinity matrix (an undirected graph) from the given data, and then obtain the final clustering results using a spectral clustering algorithm [36] such as normalized cuts (NCuts) [37]. Elhamifar and Vidal [5] proposed a sparse subspace clustering (SSC) method, which uses the sparsest representation of the data points produced by l_1 -norm minimization to define an affinity matrix of the undirected graph. Then spectral clustering techniques are used to perform subspace clustering. The convex optimization model of SSC, under the assumption that the subspaces are either linearly independent or disjoint under certain conditions, results in a block diagonal solution. However, there is no global structural constraint on the sparse representation. Moreover, SSC needs to carefully tune the number of nearest neighbors to improve performance, which leads to another parameter.

Liu et al. [4] recently introduced low-rank representation techniques into the subspace clustering problem and established a low-rank representation (LRR) algorithm [4]. LRR assumes that the data samples are approximately drawn from a mixture of multiple low-rank subspaces. The goal of LRR is to take the correlation structure of data into account, and find the lowest-rank representation of the data matrix using an appropriate dictionary. LRR solves the convex optimization problem of nuclear-norm minimization, which is considered as a surrogate for rank minimization. It performs subspace clustering excellently. However, the affinity for the spectral clustering input, which can be computed using a symmetrization step of the low-rank representation results [2], is not good at characterizing how other samples contribute to the reconstruction of a given sample. In addition, the motivation of a new version of LRR to use the matrix U^*U^{*T} as an affinity for the spectral clustering input remains vague without theoretical analysis [4]. Here, U^* can be found using the skinny SVD of the low-rank representation Z , i.e., $Z = U^*\Sigma^*V^{*T}$. Ni et al. [30] proposed a robust

low-rank subspace segmentation method to extend LRR and improve performance. It enforces the symmetric positive semi-definite (PSD) constraint to explicitly obtain a symmetric PSD matrix and avoid the symmetrization post-processing. LRR and its variations are guaranteed to produce block-diagonal affinity matrices under the independence assumption. However, non-negativity of the values of the PSD matrix cannot be guaranteed by PSD conditions. Consequently, negative elements of the PSD matrix lack physical interpretation for visual data. Besides, a pairwise affinity relationship for spectral clustering between data points inevitably leads to loss of information. This means that it does not fully capture the complexity of the problem, i.e., the intrinsic correlation of data points [38, 39]. To tackle this difficulty, one needs to learn an affinity matrix by exploiting the structure of the low-rank representation.

In this paper, we address the problem of low-rank representation-based robust subspace clustering by introducing a subspace clustering algorithm, a low-rank representation with symmetric constraint (LRRSC). LRRSC is inspired by low-rank representation techniques. In particular, our motivation is to integrate the symmetric constraint into the low-rankness property of high-dimensional data representation, to learn a symmetric low-rank matrix that preserves the subspace structures of high-dimensional data. Figure 1 shows an intuitive clustering example of three subjects to illustrate our basic idea and its effectiveness. By solving the nuclear-norm minimization problem in a simple and efficient way, we can learn a symmetric low-rank matrix. For example, given a set of data points, we represent each point as a linear combination of the others, where the low-rank coefficients should be symmetric. The symmetric effect of LRRSC guarantees weight consistency for each pair of data points, so that highly correlated data points are represented together. We provide a rigorous proof to minimize the nuclear-norm regularized least square problem with a symmetric constraint. As mentioned above, using a symmetric matrix as the input for subspace clustering may negatively affect the performance. To overcome this drawback, it is critical to investigate the intrinsically geometrical structure of the memberships of data points preserved in a symmetric low-rank representation, i.e., the angular information of the principal directions of the symmetric low-rank representation. This can improve the subspace clustering performance. An affinity that encodes the memberships of subspaces can be constructed using the angular information of the normalized rows of U^* , or columns of V^{*T} , obtained from the skinny SVD of the symmetric matrix Z , i.e., $Z = U^*\Sigma^*V^{*T}$. With the learned affinity matrix, spectral clustering can segment the data into clusters with the underlying subspaces they are drawn from. The proposed algorithm not only recovers the dimensions of each subspace, but also effectively learns a symmetric low-rank representation for the purpose of subspace clustering. In contrast to LRR, LRRSC can automatically make a coefficient matrix symmetric, and then it builds a desired affinity for subspace clustering. Further details will be discussed in Section 3.

The proposed LRRSC method provides several advantages:

- a) It incorporates the symmetry idea into low-rank representa-

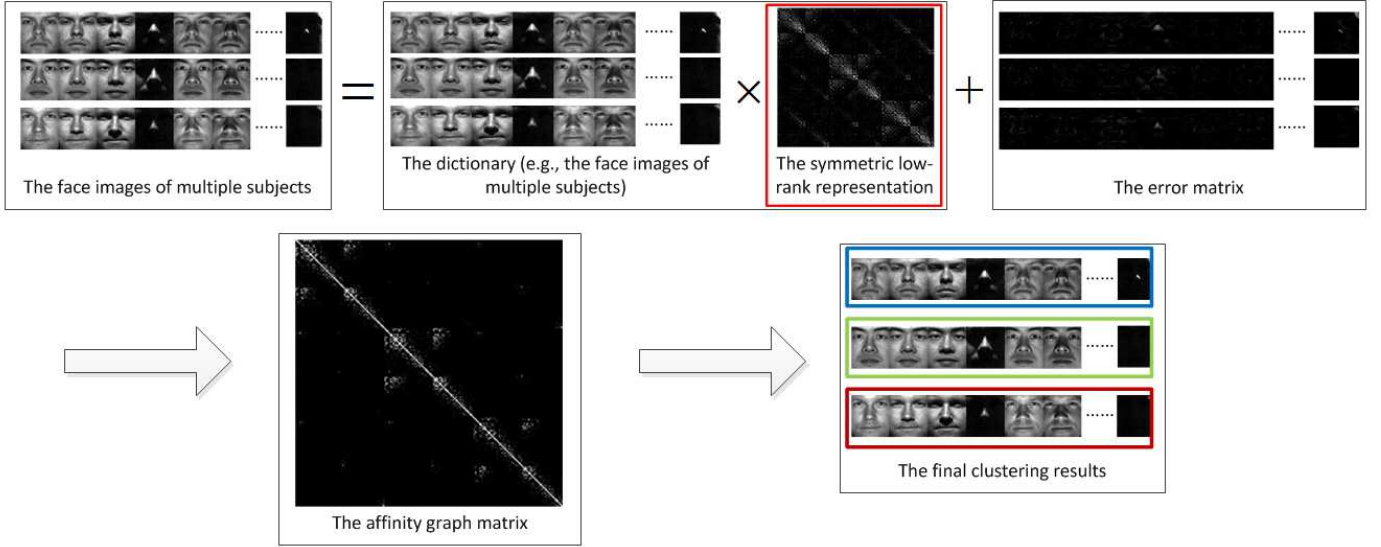


Figure 1: Illustration of the clustering problem of three subjects in the proposed method.

tion learning, and can successfully learn a symmetric low-rank matrix for high-dimensional data representation. The introduction of low-rank representation with a symmetric constraint enriches the relationship of data samples for robust subspace clustering.

- b) We have provided a rigorous proof for minimizing the nuclear-norm regularized least square problem with a symmetric constraint. This can be solved very efficiently in a closed form solution using SVD techniques.
- c) It exploits the intrinsically geometrical structure of the memberships of data points preserved in a symmetric low-rank matrix (i.e., the angular information of principal directions of the symmetric low-rank representation) to construct an affinity matrix with more separation ability. This significantly improves the subspace clustering performance.
- d) It solves the nuclear-norm minimization optimization problem with a symmetric constraint, and can be regarded as an improvement of LRR. It also inherits the advantages of LRR, which captures the global structure of data. Compared with other state-of-the-art methods, our extensive experimental results using benchmark databases demonstrate the effectiveness and robustness of LRRSC for subspace clustering

The remainder of this paper is organized as follows. Section 2 summarizes some related work on low-rank representation techniques that inspired this work. Section 3 presents the proposed LRRSC for subspace clustering. Extensive experimental results using benchmark databases are presented in Section 4. Finally, Section 5 concludes this paper.

2. A review of previous work

Consider a set of data vectors $X = [x_1, x_2, \dots, x_n] \in \mathbf{R}^{d \times n}$, each column of which is drawn from a union of k subspaces $\{S_i\}_{i=1}^k$ of unknown dimensions. The goal of subspace clustering is to

cluster data points into their respective subspaces. A main challenge in applying spectral clustering to subspace clustering is to define a good affinity matrix, each entry of which measures the similarity between data points x_i and x_j . This section provides a review of low-rank representation techniques for solving subspace clustering problems that are closely related to the proposed method.

2.1. Subspace Clustering by Low-Rank Representation

Recently, Liu et al. [4] proposed a novel objective function named the low-rank representation method for subspace clustering. Instead of seeking a sparse representation in SSC, LRR seeks the lowest-rank representation among all the candidates that can represent the data samples as linear combinations of the bases in a given dictionary. SSC enforces that Z is sparse by imposing an l_1 -norm regularization on Z , while LRR encourages Z to be low-rank using nuclear-norm regularization. By using the nuclear norm as a good surrogate for the rank function, LRR solves the following nuclear norm minimization problem for the noise free case:

$$\min_Z \|Z\|_* \quad s.t. \quad X = AZ, \quad (1)$$

where $A = [a_1, a_2, \dots, a_n] \in \mathbf{R}^{d \times n}$ is an overcomplete dictionary, and $\|\cdot\|_*$ denotes the nuclear norm (the sum of the singular values of the matrix). When the subspaces are independent, LRR succeeds in recovering the desired low-rank representations.

In the case of data being grossly corrupted by noise or outliers, the LRR algorithm solves the following convex optimization problem:

$$\min_{Z, E} \|Z\|_* + \lambda \|E\|_l \quad s.t. \quad X = AZ + E, \quad (2)$$

where $\|\cdot\|_l$ indicates a certain regularization strategy for characterizing various corruptions. For example, the $l_{2,1}$ -norm encourages the columns of E to be zero. By choosing an appropriate dictionary A , LRR seeks the lowest-rank representation

matrix. This can also be used to recover the clean data from the original samples. To reduce the computational complexity, LRR uses XP^* as its dictionary, where P^* can be computed by orthogonalizing the columns of X^T .

The above optimization problem is convex, and can be efficiently solved by the inexact augmented Lagrange multipliers (ALM) technique in polynomial time with a guaranteed high performance [19]. After obtaining an optimal solution (Z^*, E^*) , Z^* is used to define an affinity matrix $|Z| + |Z|^T$ for spectral clustering.

To avoid symmetrization post-processing, Ni et al. [30] presented an improved LRR model with PSD constraints, which can be formulated as

$$\min_{Z,E} \|Z\|_* + \lambda \|E\|_l \quad s.t. \quad X = XZ + E, Z \geq 0. \quad (3)$$

Rigorous mathematical derivations [30] show that the LRR-PSD model is equivalent to the LRR scheme, and establishes the uniqueness of the optimal solution. By applying a scheme similar to LRR, LRR-PSD can also be efficiently solved. Then, Z^* is used to define an affinity matrix $|Z|$, after acquiring an optimal solution (Z^*, E^*) .

3. Exploitation of a Low-Rank Representation with a Symmetric Constraint

In this section, we propose a low-rank representation with a symmetric constraint (LRRSC). Our approach takes into consideration the intrinsically geometrical structure of the symmetric low-rank representation of high-dimensional data. We first propose a low-rank representation model with a symmetric constraint, which can be efficiently calculated by solving a convex optimization problem. Then, we learn an affinity matrix for subspace clustering by exploiting the intrinsically geometrical structure of the memberships of data points preserved in the symmetric low-rank representation (i.e., the angular information of the principal directions of the symmetric low-rank representation). Finally, we discuss the convergence properties and present a computational complexity analysis of LRRSC.

3.1. Low-Rank Representation with Symmetric Constraint

When there are no errors in data X (i.e., the data are strictly drawn from k independent subspaces) the row space of the data, denoted by V^*V^{*T} [40] (also known as the shape interaction matrix [25]), is a block diagonal matrix that has exactly k blocks. The row space of X can be used as affinity for subspace clustering, and produces good results. It can be calculated using a closed form by computing the skinny SVD of the data matrix X , i.e., $X = U^*\Sigma^*V^{*T}$. However, real observations are often noisy. Grossly corrupted observations may reduce the performance. Low-rank representation techniques can be used to alleviate these problems [4, 30].

To guarantee weight consistency for each pair of data points, we impose a symmetric constraint on the low-rank representation. Incorporating low-rank representation with a symmetric constraint in Problem (2), we consider the following convex

optimization problem to seek a symmetric low-rank representation Z :

$$\min_{Z,E} \|Z\|_* + \lambda \|E\|_{2,1} \quad s.t. \quad X = AZ + E, Z = Z^T, \quad (4)$$

where the parameter $\lambda > 0$ is used as a trade-off between low-rankness and the effect of noise. The low-rankness criterion effectively captures the global structure of X . The low-rank constraint guarantees that the coefficients of samples coming from the same subspace are highly correlated. We assume that corruptions are "sample-specific", i.e., some data vectors are corrupted and others are not. The $l_{2,1}$ -norm is used to characterize the error term E , because it encourages the columns of E to be zero. For small Gaussian noise, $\|E\|_F^2$ is an appropriate choice. Each coefficient pair (z_{ij}, z_{ji}) denotes the interaction between data points x_i and x_j . The symmetric constraint criterion is incorporated into the low-rankness property of high-dimensional data representation so that it can effectively ensure the weight consistency for each pair of data points. Consequently, the symmetric low-rank representation, which preserves the subspace structures of high-dimensional data, ensures that highly correlated data points of subspaces are represented together.

To make the objective function in Problem (4) separable, we first convert it to the following equivalent problem by introducing an auxiliary variable J :

$$\min_{Z,E,J} \|J\|_* + \lambda \|E\|_{2,1} \quad s.t. \quad X = AZ + E, Z = J, Z = Z^T. \quad (5)$$

The augmented Lagrangian function of Problem (5) is

$$\min_{Z,E,J=J^T,Y_1,Y_2} \|J\|_* + \lambda \|E\|_{2,1} + \text{tr}[Y_1^T(X - AZ - E)] + \text{tr}[Y_2^T(Z - J)] + \frac{\mu}{2} (\|X - AZ - E\|_F^2 + \|Z - J\|_F^2), \quad (6)$$

where Y_1 and Y_2 are Lagrange multipliers, and $\mu > 0$ is a penalty parameter. The above optimization problem can be formulated as follows:

$$\min_{Z,E,J=J^T,Y_1,Y_2} \|J\|_* + \lambda \|E\|_{2,1} + \frac{\mu}{2} \left(\left\| X - AZ - E + \frac{Y_1}{\mu} \right\|_F^2 + \left\| Z - J + \frac{Y_2}{\mu} \right\|_F^2 \right). \quad (7)$$

This can be effectively solved by inexact ALM [19]. The variables J , Z and E can be updated alternately at each step, while the other two variables are fixed. The updating schemes at each iteration are:

$$\begin{aligned} J_{k+1} &= \arg \min_{J=J^T} \frac{1}{\mu} \|J\|_* + \frac{1}{2} \left\| J - \left(Z + \frac{Y_2}{\mu} \right) \right\|_F^2, \\ Z_{k+1} &= (I + A^T A)^{-1} (A^T X - A^T E + J + \frac{A^T Y_1 - Y_2}{\mu}), \\ E_{k+1} &= \arg \min E \lambda \|E\|_{2,1} + \frac{\mu}{2} \left\| E - \left(X - AZ + \frac{Y_1}{\mu} \right) \right\|_F^2. \end{aligned} \quad (8)$$

The complete procedure for solving Problem (8) is outlined in Algorithm 1. By choosing a proper dictionary A , LRRSC seeks the lowest-rank representation matrix. Because each data

point can be represented by the original data points, LRRSC uses the X as its dictionary. The last equation in Problem (8) is a convex problem and has a closed form solution. It is solved using the $l_{2,1}$ -norm minimization operator [2]. The first equation in Problem (8) is solved using the following lemma:

Algorithm 1 Solving Problem (4) by Inexact ALM

Input:

data matrix X , parameters $\lambda > 0$

Initialize: $Z = J = 0, E = 0, Y_1 = Y_2 = 0, \mu = 10^{-2}, \mu_{\max} = 10^{10}, \rho = 1.1, \varepsilon = 10^{-6}$

1: **while** not converged **do**

2: update the variables as (8);

3: update the multipliers:

$$Y_1 = Y_1 + X - XZ - E;$$

$$Y_2 = Y_2 + X - \mu(Z - J);$$

4: update the parameter μ by $\mu = \min(\rho\mu, \mu_{\max})$;

5: check the convergence conditions

$$\|X - AZ - E\|_{\infty} < \varepsilon \text{ and } \|Z - J\|_{\infty} < \varepsilon;$$

6: **end while**

Output:

Z^*, E^*

Lemma 1. Given any square matrix $Q \in \mathbf{R}^{n \times n}$, the unique closed form solution to the optimization problem

$$W^* = \arg \min_W \frac{1}{\mu} \|W\|_* + \frac{1}{2} \|W - Q\|_F^2, W = W^T, \quad (9)$$

takes the form

$$W^* = U_r(\Sigma_r - \frac{1}{\mu} \cdot I_r)V_r^T, \quad (10)$$

where $\tilde{Q} = U\Sigma V^T$ is the SVD of the symmetric matrix $\tilde{Q} = (Q + Q^T)/2$, $\Sigma_r = \text{diag}(\sigma_1, \sigma_2, \dots, \sigma_r)$ where $\{r : \sigma_r > \frac{1}{\mu}\}$ are positive singular values, U_r and V_r are the corresponding singular vectors of the matrix \tilde{Q} , and I_r is an $r \times r$ identity matrix.

The proof of Lemma 1 is based on the following three lemmas.

Lemma 2. ([4] Lemma 7.1) Let U, V and W be matrices with compatible dimensions. Suppose both U and V have orthogonal columns, i.e., $U^T U = I$ and $V^T V = I$. Then we have

$$\|W\|_* = \|UWV^T\|_*. \quad (11)$$

Note that a similar equality also holds for the square of the Frobenius norm, $\|\cdot\|_F^2$.

Lemma 3. ([2] Lemma 3.1) Let A and D be square matrices, and let B and C be matrices with compatible dimensions. Then,

for any block partitioned matrix $X = \begin{bmatrix} A & B \\ C & D \end{bmatrix}$,

$$\left\| \begin{pmatrix} A & B \\ C & D \end{pmatrix} \right\|_* \geq \left\| \begin{pmatrix} A & 0 \\ 0 & D \end{pmatrix} \right\|_* = \|A\|_* + \|D\|_*. \quad (12)$$

Note that a similar inequality also holds for the square of the Frobenius norm, $\|\cdot\|_F^2$ [30].

Lemma 4. ([15, 41–43]) Let $A \in \mathbf{R}^{m \times n}$ be a given matrix and $\|\cdot\|_1$ be the l_1 -norm. The proximal operator of

$$\min_x \frac{1}{2} \|Ax - b\|_2^2 + \gamma \|x\|_1 \quad (13)$$

is $S_\gamma(x)$, i.e. the soft-thresholding operator

$$S_\gamma(x) = \begin{cases} x - \gamma, & x > \gamma \\ x + \gamma, & x < -\gamma \\ 0, & \text{else} \end{cases}.$$

Proof. (of Lemma 1) Let W^* be the unique minimizer. Then,

$$\begin{aligned} \|W^* - Q\|_F^2 &= \frac{1}{2} \left(\|W^* - Q\|_F^2 + \|W^* - Q^T\|_F^2 \right) \\ &= \frac{1}{2} \left(\|W^* - (Q + Q^T)/2\|_F^2 \right) + F(Q), \end{aligned} \quad (14)$$

where $F(Q)$ are entirely independent of W^* . Therefore, the original optimization can be converted to

$$W^* = \arg \min_W \frac{1}{\mu} \|W\|_* + \frac{1}{2} \|W - \tilde{Q}\|_F^2, W = W^T, \quad (15)$$

where $\tilde{Q} = (Q + Q^T)/2$.

Let $\tilde{Q} = U_r \Sigma_r V_r^T$ be the skinny SVD of a given symmetric matrix \tilde{Q} of rank r , where $\Sigma_r = \text{diag}(\sigma_1, \sigma_2, \dots, \sigma_r)$ and $\{\sigma_i\}_{i=1}^r$ are positive singular values. More precisely, both U_r and V_r have orthogonal columns, i.e., $U_r^T U_r = I$ and $V_r^T V_r = I$. Let $W = U_r \tilde{W} V_r^T$. By Lemma 2, Problem (15) is equivalent to

$$\tilde{W}^* = \arg \min_{\tilde{W}} \frac{1}{\mu} \|\tilde{W}\|_* + \frac{1}{2} \|\tilde{W} - \Sigma_r\|_F^2, \tilde{W} = \tilde{W}^T. \quad (16)$$

Let \tilde{W}^* be an optimizer of Problem (16), then \tilde{W}^* must be a diagonal matrix. Assume \tilde{W}_0 is a non-diagonal matrix, i.e., there exists nonzero entries in the non-diagonal of \tilde{W}^* . Let $f(\tilde{W}) = \frac{1}{\mu} \|\tilde{W}\|_* + \frac{1}{2} \|\tilde{W} - \Sigma_r\|_F^2$. By Lemma 3 and the strict decreasing property of the square of the Frobenius norm, we can always derive \tilde{W}_1 by removing the non-diagonal entries of \tilde{W}_0 such that $f(\tilde{W}_1) < f(\tilde{W}_0)$. This contradicts the non-diagonal matrix assumption.

Let $\tilde{W} = \text{diag}(w_1, w_2, \dots, w_r)$. For diagonal matrices, the sum of the singular values is equal to the sum of the absolute values of the diagonal elements, i.e., the l_1 -norm. The optimization of Problem (16) is equivalent to

$$\tilde{W}^* = \arg \min_{\tilde{W}} \frac{1}{\mu} \|\tilde{W}\|_1 + \frac{1}{2} \|\tilde{W} - \Sigma_r\|_F^2, \tilde{W} = \tilde{W}^T. \quad (17)$$

By Lemma 4, the optimal solution to this problem is given by $\tilde{W}^* = S_{\frac{1}{\mu}}(\Sigma_r)$. Finally, we get $W^* = U_r(\Sigma_r - \frac{1}{\mu} \cdot I_r)V_r^T$. \square

3.2. Building an Affinity Graph based on the Symmetric Low-rank Matrix

Using the optimal symmetric low-rank matrix Z^* from Problem (4), we need to construct an affinity graph $G = (V, E)$ associated with the corresponding adjacency matrix $W = \{w_{ij}|i, j \in$

V }, where $V = \{v_1, v_2, \dots, v_n\}$ is a set of vertices and $E = \{e_{ij}|i, j \in V\}$ is a set of edges. Note that $\{w_{ij}\}$ represents the weight of edge e_{ij} that associates vertices i and j . A fundamental problem involving affinity graph construction is how to determine the adjacency matrix W . Because each sample is represented by the others, each element z_{ij} of the matrix Z^* naturally characterizes the contribution of the sample x_j to the reconstruction of sample x_i . A straightforward method is to use the symmetric low-rank matrix Z^* as the adjacency matrix W for spectral clustering. However, in practice, the matrix Z^* cannot adequately represent the relationship between samples when there are grossly corrupted observations. Therefore, the straightforward use of the matrix Z^* as a pairwise affinity relationship between data points inevitably results in loss of information, and it does not fully capture the intrinsic correlation of data points [38, 39]. Consequently, the clustering performance may seriously decline because of a lack of robustness.

To enhance the ability of the low-rank representation to separate samples in different subspaces, a reasonable strategy is to derive an affinity graph with enhanced clustering information from the matrix Z^* . This preserves the subspace structures of high-dimensional data, and recovers the clustering relations among samples. Instead of directly using $|Z^*| + |(Z^*)^T|$ to define an affinity graph, we consider the mechanism driving the construction of the affinity graph from the matrix Z^* . We consider Z^* with the skinny SVD $U^* \Sigma^* (V^*)^T$. Note that U^* and V^* are the orthogonal bases of the column and row space of the matrix Z^* . Inspired by [4, 31], we assign each column of U^* a weight by multiplying it by $(\Sigma^*)^{1/2}$, and each row of $(V^*)^T$ a weight by multiplying it by $(\Sigma^*)^{1/2}$. Then, we can define $M = U^* (\Sigma^*)^{1/2}$, $N = (\Sigma^*)^{1/2} (V^*)^T$. The product of two matrices can represent Z^* , i.e., $Z^* = MN$.

Because Z^* is a symmetric low-rank matrix, the absolute values of the columns of U^* and V^* always agree. The columns of U^* or V^* can span the principal directions of the symmetric low-rank matrix Z^* , and the diagonal entries reflect the relative importance of the coefficient matrix Z^* in each of these directions. Therefore, we use angular information from all of the row vectors of matrix M , or all of the column vectors of matrix N , instead of Z^* , to define an affinity matrix W as follows:

$$[W]_{ij} = \left(\frac{m_i^T m_j}{\|m_i\|_2 \|m_j\|_2} \right)^{2\alpha} \quad \text{or} \quad [W]_{ij} = \left(\frac{n_i^T n_j}{\|n_i\|_2 \|n_j\|_2} \right)^{2\alpha}, \quad (18)$$

where m_i and m_j denote the i -th and j -th row of the matrix M , or n_i and n_j denote the i -th and j -th column of the matrix N . The values of the affinity matrix W can be distributed on the unit ball by the l_2 -norm of data vectors. Consequently, the affinity matrix W preserves angular information between data vectors but removes length information. By using $(\cdot)^{2\alpha}$ we ensure that the values of the affinity matrix W are positive inputs for the subspace clustering, and also increase the separation of points of different groups because of the geometry of the l_2 -norm ball. Finally, we apply spectral clustering algorithms such as NCuts [37] to segment the samples into a given number of clusters. Algorithm 2 summarizes the complete subspace clustering algorithm of LRRSC.

Algorithm 2 The LRRSC algorithm

Input:

data matrix $X = [x_1, x_2, \dots, x_n] \in \mathbf{R}^{m \times n}$, number k of subspaces, regularized parameters $\lambda > 0, \alpha > 0$

1: Solving the following problem by Algorithm 1:

$$\min_{Z, E} \|Z\|_* + \lambda \|E\|_{2,1} \quad \text{s.t.} \quad X = AZ + E, Z = Z^T,$$

and obtain the optimal solution (Z^*, E^*) .

2: Compute the skinny SVD $Z^* = U^* \Sigma^* (V^*)^T$.

3: Calculate $M = U^* (\Sigma^*)^{1/2}$ or $N = (\Sigma^*)^{1/2} (V^*)^T$.

4: Construct the affinity graph matrix W , i.e.,

$$[W]_{ij} = \left(\frac{m_i^T m_j}{\|m_i\|_2 \|m_j\|_2} \right)^{2\alpha} \quad \text{or} \quad [W]_{ij} = \left(\frac{n_i^T n_j}{\|n_i\|_2 \|n_j\|_2} \right)^{2\alpha}.$$

5: Apply W to perform NCuts.

Output:

The clustering results.

3.3. Convergence properties and computational complexity analysis

The convergence properties of the exact ALM algorithm for a smooth objective function have been generally proven in [19]. The inexact variation of ALM has been extensively studied and generally converges well. Algorithm 2 performs well in practical applications. We assume that the size of X is $m \times n$, where X has n samples and each sample has m dimensions. The computational complexity of the first step in Algorithm 1 is $O(n^3)$ because it requires computing the SVD of a $n \times n$ matrix. The overall computational complexity of Algorithm 1 is $O(2n^3 + mn^2)$. When $n > m$, the computational complexity of Algorithm 1 can be considered to be $O(n^3)$. The computational complexity of Algorithm 2 is $O(m^3) + O(n^3)$, where t is the number of iterations. Therefore, the final overall complexity of Algorithm 2 is $O(m^3)$. In our experiments, there were always less than 335 iterations.

4. Experiments

In this section, we evaluated the performance of the proposed LRRSC algorithm using a series of experiments on publicly available databases, the extended Yale B and Hopkins 155 databases (the Matlab source code of our method is available at <http://www.machineilab.org/users/chenjie>). We compared the performance of LRRSC with several state-of-the-art subspace clustering algorithms (LRR [4], LRR-PSD [30], SSC [5], low rank subspace clustering (LRSC) [6, 7] and local subspace affinity (LSA) [8]). As there is no source code publicly available for LRR-PSD, we implemented the LRR-PSD algorithm according to its theory. For the other algorithms, we used the source codes provided by their authors.

We use the subspace clustering error as a measure of performance,

$$\text{error} = \frac{N_{\text{error}}}{N_{\text{total}}}, \quad (19)$$

Table 1: Parameter settings of different algorithms. The parameter λ is used as a trade-off between low rankness (or sparsity) and the effect of noise (LRRSC, LRR, LRR-PSD, SSC). The parameter α enhances the separate ability of low-rank representation between samples in different subspaces used by LRRSC. For LSA, K is number of nearest neighbors and d is dimension to fit local subspaces. For LRSC, τ and λ are two parameters weighting noise.

Method	Face clustering		Motion segmentation	
	Scenario 1	Scenario 2	Scenario 1	Scenario 2
LRRSC	$\lambda = 0.2, \alpha = 4$	$\lambda = 0.1, \alpha = 3$	$\lambda = 3.3, \alpha = 2$	$\lambda = 3, \alpha = 3$
LRR	$\lambda = 0.18$		$\lambda = 4$	
LRR-PSD	$\lambda = 0.08$		$\lambda = 4$	
SSC	$\lambda_e = 8/\mu_e$	$\lambda_e = 20/\mu_e$	$\lambda_z = 800/\mu_z$	
LSA	$K = 3, d = 5$		$K = 8, d = 5$	$K = 8, d = 4$
LRSC	$\tau = 0.4, \alpha = 0.045$	$\tau = 0.045, \alpha = 0.045$	$\tau = 420, \alpha = 3000$ or $\alpha = 5000$	

where N_{error} represents the number of misclassified points, and N_{total} is the total number of points. LRRSC has two parameters, λ and α . Empirically speaking, the parameter λ should be relatively large if the data are "clean", or smaller if they are contaminated with small noises, and the parameter α ranges from 2 to 4. For the other algorithms, we used the parameters given by the respective authors, or manually tuned the parameters to find the best results. The parameters for these methods are shown in Table 1. For LRR, we post-processed the affinity matrix [4]. For LRSC, we chose the noisy data version of (P_3) as its instance. All the experiments are implemented on Windows 7 and Matlab R2011b, which are performed on a personal computer with Intel Core i5-2300 CPU and 16GB memory.

4.1. Experiments on face clustering

Given a collection of face images from multiple individuals, the face clustering problem clusters images according to their individuals. It has been shown that images of an individual's face with variations such as illumination and expression changes can be well approximated by a low-dimensional subspace [13]. The set of face images from multiple individuals lie close to a union of 9-dimensional subspaces [13]. Hence, the problem of face clustering reduces to clustering a collection of images in a union of subspaces.

In this section, we consider the Extended Yale B Database [44, 45] for the face clustering problem. The extended Yale B database consists of 2414 frontal images from 38 individuals. There are approximately 59 – 64 images available for each person, captured under various laboratory-controlled lighting conditions. Fig. 2 shows some sample images. We considered two different experimental scenarios to evaluate the performance of our proposed method for face clustering. To reduce the computational time and memory requirements of the algorithms, we resized the images to 48×42 pixels.



Figure 2: Example images from the Extended Yale B database in our experiments.

1. **First experimental scenario:** We used the first 10 classes of the Extended Yale B Database, as in [2]. This subset of the database contains 640 frontal face images from

10 subjects. To compare the clustering errors between different approaches, we first used the raw pixel values without pre-processing, considering each image as a data vector of 2016 dimensions. Then, we applied PCA to pre-process these face images using 100 and 500 feature dimensions.

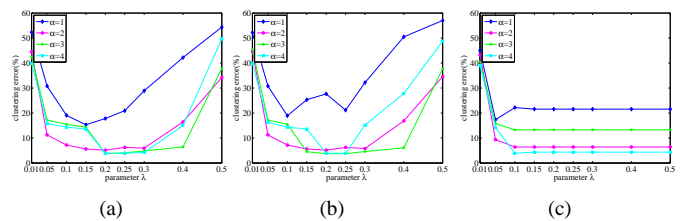


Figure 3: Changes in clustering error when varying λ and α , using the first 10 classes in the Extended Yale B Database. (a) Raw data. (b) The 500-dimensional data obtained by applying PCA. (c) The 100-dimensional data obtained by applying PCA.

Fig. 3 shows the influence of the parameters λ and α on the face clustering errors of LRRSC. In each experiment, $\alpha \in \{1, 2, 3, 4\}$. Larger α led to a better clustering performance. For example, we let λ range from 0.15 to 0.4 with $\alpha = 3$. Then, the clustering error varied from 3.91% to 6.41% (Fig. 3(a)). When we let λ range from 0.15 to 0.4 with $\alpha = 1$, the clustering error varied from 15.31% to 42.19%. However, note that if α is too large (i.e., $\alpha = 4$) LRRSC must narrow the range of parameter λ to obtain the desired result. This can also be observed in Fig. 3(b). Fig. 3(c) shows that LRRSC performs well for a large range of λ . This is because of the 100-dimensional data obtained by applying PCA with noise removal. Consequently, LRRSC is capable of a stable face clustering performance when λ is chosen according to the noise level.

Table 2: Clustering error (%) of different algorithms on the first 10 classes of the Extended Yale B Database.

Algorithm	LRRSC	LRR	LRR-PSD	SSC	LSA	LRSC
Dim. = 100	4.37	21.09	38.44	36.56	64.22	35.78
Dim. = 500	3.91	21.56	35.47	35	61.25	35.78
Raw data	3.91	20.94	35.47	35	59.52	35.78

The three different feature dimensions of the face images required 32, 114 and 113 iterations. Table 2 shows the face clustering results of different algorithms in the first experimental scenario. It is clear that our proposed LRRSC method has lower clustering errors than the other algorithms. For example,

our method improved the clustering accuracy by at least 17% when compared with the other algorithms, and achieved a low clustering error of 3.91% for the original data. We observed the same advantages when using our proposed method for the 500- and 100-dimensional data obtained using PCA. The clustering results for each algorithm using raw or reduced dimension data are very similar, which demonstrates that the face images of an individual lie close to a union of subspaces. These clustering results confirmed that the affinity calculated from the symmetric low-rank representation significantly improves the clustering accuracy when the data are grossly contaminated by noise, and that it outperforms the other algorithms. LRR compares favorably against the other algorithms. LRR-PSD, SSC, and LRSC have very similar clustering results. LSA does not perform well, even with the original data. This is because LSA is very sensitive to large errors, and does not have an explicit way to deal with corrupted data.

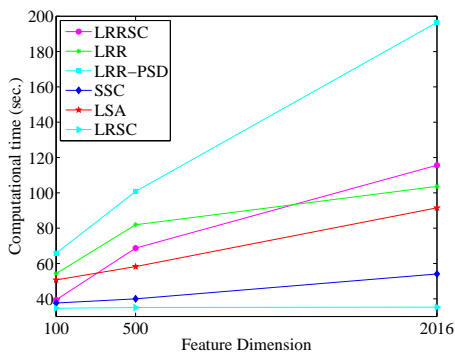


Figure 4: Computational time (seconds) of each algorithm for different feature dimensions, using the first 10 classes of the Extended Yale B Database.

From the computational times shown in Fig. 4, we can see that LRSC significantly outperformed the other approaches. This is because LRSC can obtain a closed form solution of the low-rank representation, which it uses to build the affinity. Thus, it can run much faster than the other approaches. On other hand, LRRSC, LRR, SSC have comparable computational times because of their efficient convex optimization techniques.

2. **Second experimental scenario:** We used the experimental settings from [5]. We divided the 38 subjects into four groups, where subjects 1 to 10, 11 to 20, 21 to 30, and 31 to 38 correspond to four different groups. For each of the first three groups, we considered all choices of $n \in \{2, 3, 5, 8, 10\}$. For the last group, we considered all choices of $n \in \{2, 3, 5, 8\}$. We tested each choice (i.e., each set of n subjects) using each algorithm. Finally, the mean and median subspace clustering errors for different numbers of subjects were computed using all algorithms. Note that we applied these clustering algorithms to the normalized face images.

Table 3 shows the clustering results of various approaches using different numbers of subjects. When considering two subjects, LRRSC and SSC obtained very similar results and achieved a clustering error of nearly 1.8%. This was the best among the other algorithms. Nevertheless, the LRRSC al-

Table 3: Average clustering error (%) for different numbers of subjects, applying each algorithm to the Extended Yale B database.

Algorithm	LRRSC	LRR	LRR-PSD	SSC	LSA	LRSC
2 Subjects						
Mean	1.78	2.54	3.04	1.86	41.97	4.25
Median	0.78	0.78	2.34	0	47.66	3.13
3 Subjects						
Mean	2.61	4.23	4.33	3.24	56.62	6.07
Median	1.56	2.6	3.91	1.04	61.98	5.73
5 Subjects						
Mean	3.19	6.92	10.45	4.33	59.29	10.19
Median	2.81	5.63	7.19	2.82	56.25	7.5
8 Subjects						
Mean	4.01	13.62	23.86	5.87	57.17	23.65
Median	3.13	9.67	28.61	4.49	59.38	27.83
10 Subjects						
Mean	3.7	14.58	32.55	7.29	59.38	31.46
Median	3.28	16.56	34.06	5.47	60.94	28.13

gorithm consistently obtained lower clustering errors than the other algorithms when the number of subjects increased. For example, there was at least 3.6% improvement in clustering accuracy compared with SSC for 10 subjects. Note that SSC performed better than the other low-rank based representation approaches (LRR, LRR-PSD, and LRSC) in terms of the clustering error. This confirms that our proposed method is very effective and robust to different number of subjects for face clustering.

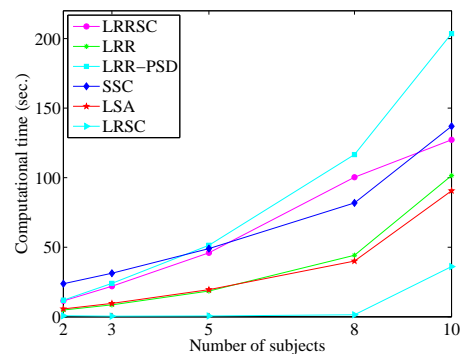


Figure 6: Comparison of mean computational time (seconds) of each algorithm applied to the Extended Yale B database, using different numbers of subjects.

Fig. 5 shows examples of the affinity graph matrix produced by the different algorithms for the Extended Yale B Database with five subjects. It is clear from Fig. 5 that the affinity graph matrix produced by LRRSC has a distinct block-diagonal structure, whereas the other approaches do not. The clear block-diagonal structure implies that each subject becomes highly compact and the different subjects are better separated. Note that the number of iterations taken by our algorithm is always less than 335. The average numbers of iterations for the five different sets ($n \in \{2, 3, 5, 8, 10\}$ subjects) in the proposed method are 308, 256, 202, 182 and 166.

Fig. 6 shows the mean computational times for the Extended Yale B database with different numbers of subjects. Note that

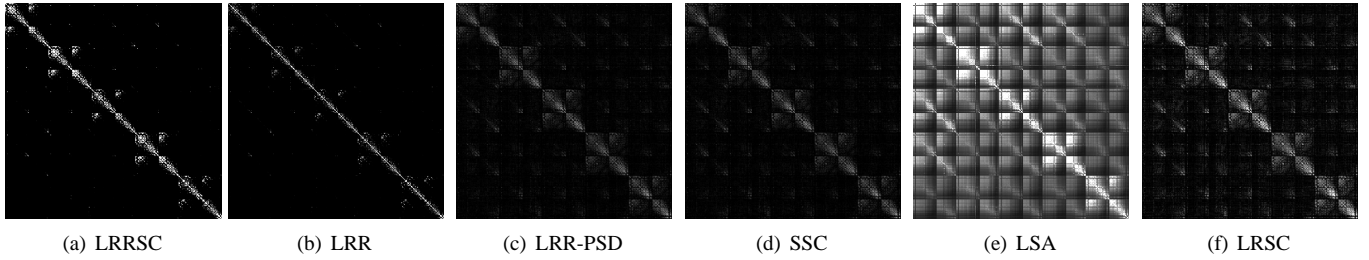


Figure 5: Examples of the affinity graph matrix produced when using different algorithms for the Extended Yale B Database with five subjects.

the computational time of LRSC is still much lower than the other algorithms. However, LRSC does not perform well, especially as the number of subjects increases. LRRSC, LRR, SSC, and LSA have comparable computational times in these experiments.

4.2. Experiments on motion segmentation

Motion segmentation refers to the problem of segmenting feature trajectories of multiple rigidly moving objects into their corresponding spatiotemporal regions in a video sequence. The feature trajectories from a single rigid motion lie in a linear subspace of at most four dimensions [14]. Motion segmentation can be regarded as a subspace clustering problem. We consider the Hopkins 155 motion database [46] for the motion segmentation problem. It consists of 156 sequences of two motions or three motions. Fig. 7 shows some example frames from two video sequences with traced feature points. There are 39 – 550 data vectors drawn from two or three motions for each sequence, which correspond to a subspace. Each sequence is a separate clustering task.



Figure 7: Example frames from two video sequences with traced feature points involving three motions.

We considered two scenarios to evaluate the performance of the applicability of the LRRSC algorithm to motion segmentation. We first used the original feature trajectories associated with each motion in an affine subspace, i.e., enforced that the coefficients sum to 1. Then, we projected the original data into a $4n$ -dimensional subspace using PCA, where n is the number of subspaces.

The clustering performance for all 156 sequences was largely affected by λ . Fig. 8(a) and 8(b) show the clustering errors of LRRSC using two experimental settings for different λ over all 156 sequences. In Fig. 8(a), when λ was between 1 and 6 the clustering error varied between 1.5% and 2.67%; when λ was between 2.4 and 4, the clustering error remained very

stable, varying between 1.5% and 1.7%. In Fig. 8(b), when λ was between 1 and 6, the clustering error varied from 1.56% to 3.18%; when λ was between 2.4 and 4, the clustering error varied from 1.56% to 2.31% and remained very stable. This implies that LRRSC performs well under a wide range of values of λ . In addition, choosing λ for each sequence may improve the clustering performance, especially when the data are grossly corrupted by noise.

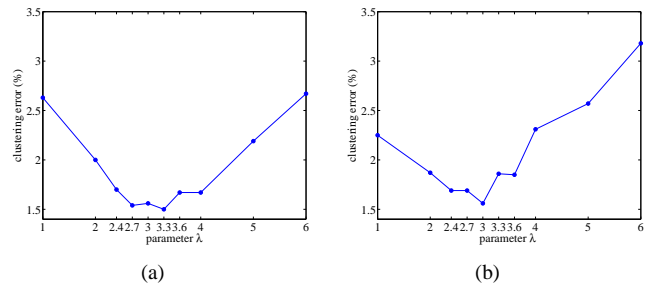


Figure 8: The influences of the parameter λ of LRRSC. (a) The clustering error of LRRSC on the Hopkins 155 database with the $2F$ -dimensional data points. (b) The clustering error of LRRSC on the Hopkins 155 database with the $4n$ -dimensional data points obtained by applying PCA.

Table 4 and 5 show the average clustering errors of the different algorithms on all 156 sequences of the Hopkins 155 database, using two experimental settings. We note that the accuracy of LRRSC was very similar for the two experimental settings. This confirms that the feature trajectories of each sequence in a video approximately lie close to a $4n$ -dimensional linear subspace of the $2F$ -dimensional ambient space [14]. In both experimental settings, LRRSC obtained competitive clustering results and significantly outperformed the other algorithms. Specifically, LRRSC obtained 1.5% and 1.56% clustering errors for the two experimental settings. This confirms the effectiveness and robustness of LRRSC for the segmentation of different motion subspaces by exploiting the angular information of the principal directions of the symmetric low-rank representation of each motion. Note that LRR and SSC perform better than LRR-PSD, LSA, and LRSC, and are effective and robust methods for motion segmentation. The computational cost of LRSC is much lower than the other algorithms. The computational cost of LRR is lower than the low-rank representation based methods (LRRSC and LRR-PSD). This is because LRR applies the dictionary learning method to improve performance, while LRRSC uses one SVD computation at each

iteration and the original data’s dictionary.

Table 4: Average clustering error (%) and mean computation time (seconds) when applying the different algorithms to the Honkins 155 database, with the $2F$ -dimensional data points.

Algorithm	Error				Time
	mean	median	std.	max.	
LRRSC	1.5	0	4.36	33.33	4.71
LRR	1.71	0	4.86	33.33	1.29
LRR-PSD	5.38	0.55	10.18	45.79	4.35
SSC	2.23	0	7.26	47.19	1.02
LSA	11.11	6.29	13.04	51.92	3.44
LRSC	4.73	0.59	8.8	40.55	0.14

Table 5: Average clustering error (%) and mean computation time (seconds) when applying the different algorithms to the Honkins 155 database, with the $4n$ -dimensional data points obtained using PCA.

Algorithm	Error				Time
	mean	median	std.	max.	
LRRSC	1.56	0	5.48	43.38	4.62
LRR	2.17	0	6.58	43.38	0.69
LRR-PSD	5.78	0.57	10.6	45.79	5.23
SSC	2.47	0	7.5	47.19	0.93
LSA	4.7	0.6	10.2	54.51	3.35
LRSC	4.89	0.63	8.91	40.55	0.13

5. Conclusions

In this paper, we proposed a method that used a low-rank representation with a symmetric constraint to solve the problem of subspace clustering, using an assumption that high-dimensional data are approximately drawn from a union of multiple subspaces. In contrast with existing low-rank based algorithms, LRRSC integrates the symmetric constraint into the low-rankness property of high-dimensional data representation, which can be efficiently calculated by solving a convex optimization problem. The affinity matrix for spectral clustering can be obtained by further exploiting the angular information of the principal directions of the symmetric low-rank representation. This is a critical step towards understanding the memberships between high-dimensional data points. Extensive experiments on benchmark databases showed that LRRSC produces very competitive results for subspace clustering compared with several state-of-the-art subspace clustering algorithms, and demonstrated its robustness when handling noisy real-world data.

Low-rank representation based techniques such as LRR and LRRSC have the advantage (when compared with sparsity based methods) of being able to capture globally linear structures of data. However, there are still several significant problems. Although the parameter α of LRRSC can be easily chosen empirically because it has a limited range, it is difficult to estimate the parameter λ without prior knowledge. In addition, it is important to develop dictionary learning algorithms, because a proper learned dictionary may significantly improve the subspace clustering performance. Moreover, LRRSC involves

one SVD computation at each iteration, and hundreds of iterations are required for convergence. Therefore, it suffers from a high computation cost because multiple iterations are needed, and the SVD computations in these iterative processes on large matrices are prohibitive. In future work, we will also focus on speeding up the optimization problems for practical applications.

Acknowledgments

The authors thank the anonymous reviewers for their thorough and valuable comments and suggestions.

References

- [1] W. Hong, J. Wright, K. Huang, Y. Ma, Multiscale hybrid linear models for lossy image representation, *IEEE Trans. Image Processing* 15 (2006) 3655–3671.
- [2] G. Liu, Z. Lin, Y. Yu, Robust subspace segmentation by low-rank representation, In *ICML* (2010).
- [3] J. Ho, M. Yang, J. Lim, K. Lee, Clustering appearances of objects under varying illumination conditions, In *CVPR* (2003).
- [4] G. Liu, Z. Lin, S. Yan, J. Sun, Y. Yu, Y. Ma, Robust recovery of subspace structures by low-rank representation, *IEEE Trans. Pattern Anal. and Mach. Intell.* 35 (2013) 171–184.
- [5] E. Elhamifar, R. Vidal, Sparse subspace clustering algorithm, theory, and applications, *IEEE Trans. Pattern Anal. and Mach. Intell.* 35 (2013) 2765–2781.
- [6] P. Favarob, R. Vidala, A closed form solution to robust subspace estimation and clustering, In *CVPR* (2011).
- [7] R. Vidala, P. Favarob, Low rank subspace clustering (LRSC), *Pattern Recognition Letters* (2013).
- [8] J. Yan, M. Pollefeys, A general framework for motion segmentation: Independent, articulated, rigid, non-rigid, degenerate and non-degenerate, In *European Conf. on Computer Vision* (2006) 94–106.
- [9] S. Rao, R. Tron, R. Vidal, Y. Ma, Motion segmentation in the presence of outlying, incomplete, or corrupted trajectories, *IEEE Trans. Pattern Anal. and Mach. Intell.* 32 (2010) 1832–1845.
- [10] L. Zappella, X. Lladò, E. Provenzi, J. Salvi, Enhanced local subspace affinity for feature-based motion segmentation, *Pattern Recognition* 44 (2011) 454–470.
- [11] D. Pham, S. Budhaditya, D. Phung, S. Venkatesh, Improved subspace clustering via exploitation of spatial constraints, In *CVPR* (2012) 550–557.
- [12] L. Zhuang, H. Gao, Z. Lin, Y. Ma, X. Zhang, N. Yu, Non-negative low rank and sparse graph for semi-supervised learning, In *CVPR* (2012).
- [13] R. Basri, D. W. Jacobs, Lambertian reflectance and linear subspaces, *IEEE Trans. Pattern Anal. and Mach. Intell.* 25 (2003) 218–233.
- [14] T. Boult, L. Brown, Factorization-based segmentation of motions, in *IEEE Workshop on Proceedings of the Visual Motion* (1991) 179–186.
- [15] R. Tibshiran, Regression shrinkage and selection via the lasso, *Journal of the Royal Statistical Society Series B* 58 (1996) 267–288.
- [16] D. Donoho, For most large underdetermined systems of linear equations the minimal l_1 -norm solution is also the sparsest solution, *Comm. Pure and Applied Math.* 59 (2006) 797–829.
- [17] J. Wright, A. Ganesh, S. Rao, Y. Peng, Y. Ma, Robust principal component analysis: Exact recovery of corrupted low-rank matrices by convex optimization, In *NIPS* (2009) 2080–2088.
- [18] E. J. Candès, Y. Plan, Matrix completion with noise, *Proceedings of the IEEE* 6 (98) 925–936.
- [19] Z. Lin, M. Chen, Y. Ma, The augmented lagrange multiplier method for exact recovery of corrupted low-rank matrices, *arXiv preprint arXiv:1009.5055* (2011).
- [20] E. J. Candès, X. Li, Y. Ma, J. Wright, Robust principal component analysis, *Journal of the ACM (JACM)* 58 (2011).
- [21] Z. Lin, R. Liu, Z. Su, Linearized alternating direction method with adaptive penalty for low-rank representation, *arXiv preprint arXiv:1109.0367* (2012).

- [22] I. Jolliffe, *Principal Component Analysis*, Springer New York, 2002.
- [23] R. Vidal, Subspace clustering, *Signal Processing Magazine, IEEE* 28 (2011) 52–68.
- [24] M. Fischler, R. Bolles, Random sample consensus: a paradigm for model fitting with applications to image analysis and automated cartography, *Communications of the ACM* 24 (1981) 381–395.
- [25] J. P. Costeira, T. Kanade, A multibody factorization method for independently moving objects, *Int. J. Comput. Vision* 29 (1998) 159–179.
- [26] V. Govindu, A tensor decomposition for geometric grouping and segmentation, In *CVPR* (2005).
- [27] A. Shashua, R. Zass, T. Hazan, Multi-way clustering using super-symmetric non-negative tensor factorization, In *ECCV* (2006).
- [28] R. Vidal, Y. Ma, S. Sastry, Generalized principal component analysis (GPCA), *IEEE Trans. Pattern Anal. and Mach. Intell.* 27 (2005) 1945–1959.
- [29] J. Ho, M. Y. J. Lim, K. Lee, D. Kriegman, Clustering appearances of objects under varying illumination conditions, In *CVPR* (2003).
- [30] Y. Ni, J. Sun, S. Y. X. Yuan, L. Cheong, Robust low-rank subspace segmentation with semidefinite guarantees, *Proceedings of the IEEE International Conference on Data Mining Workshops (ICDMW)* (2010) 1179–1188.
- [31] F. Lauer, C. Schnörr, Spectral clustering of linear subspaces for motion segmentation, in *IEEE International Conference on Computer Vision* (2009) 678–685.
- [32] E. J. Candès, M. B. Wakin, S. P. Boyd, Enhancing sparsity by reweighted l_1 minimization, *Journal of Fourier Analysis and Applications* 14 (2008) 877–905.
- [33] B. Recht, M. Fazel, P. Parrilo, Guaranteed minimum-rank solutions of linear matrix equations via nuclear norm minimization, *SIAM review* 52 (2010) 471–501.
- [34] J.-F. Cai, E. J. Candès, Z. Shen, A singular value thresholding algorithm for matrix completion, *SIAM J. on Optimization* 20 (2010) 1956–1982.
- [35] K. Toh, S. Yun, An accelerated proximal gradient algorithm for nuclear norm regularized linear least squares problems, *Pacific Journal of Optimization* 15 (2010) 615–640.
- [36] U. V. Luxburg, A tutorial on spectral clustering, *Statistics and computing* 17 (2007) 395–416.
- [37] J. Shi, J. Malik, S. Sastry, Normalized cuts and image segmentation, *IEEE Trans. Pattern Anal. and Mach. Intell.* 22 (2000) 888–905.
- [38] S. Agarwal, J. Lim, L. Zelnik-Manor, P. Perona, D. Kriegman, S. Belongie, Beyond pairwise clustering, in *CVPR* (2005).
- [39] D. Zhou, J. Huang, B. B. Schölkopf, Learning with hypergraphs: Clustering, classification, and embedding, in *Neural Information Processing Systems* (2006) 1601–1608.
- [40] S. Wei, Z. Lin, Analysis and improvement of low rank representation for subspace segmentation, *arXiv:1107.1561* (2011).
- [41] S. S. Chen, D. L. Donoho, M. A. Saunders, Atomic decomposition by basis pursuit, *SIAM Rev.* 43 (2001) 129–159.
- [42] E. T. Hale, W. Yin, Y. Zhang, Fixed-point continuation for l_1 -minimization: Methodology and convergence, *SIAM Journal on Optimization* 19 (2008) 1107–1130.
- [43] N. Parikh, S. Boyd, Proximal algorithms, *Foundations and Trends in Optimization* (2013) 1–96.
- [44] K. Lee, J. Ho, D. Kriegman, Acquiring linear subspaces for face recognition under variable lighting, *IEEE Trans. Pattern Anal. and Mach. Intell.* 27 (2005) 684–698.
- [45] A. Georghiades, P. Belhumeur, D. Kriegman, From few to many: Illumination cone models for face recognition under variable lighting and pose, *IEEE Trans. Pattern Anal. and Mach. Intell.* 23 (2011) 643–660.
- [46] R. Tron, R. Vidal, A benchmark for the comparison of 3-d motion segmentation algorithms, In *CVPR* (2007).